RGD targeted poly(*L*-glutamic acid)-cystamine-(Gd-DO3A) conjugate for detecting angiogenesis biomarker $\alpha_v\beta_3$ integrin with MR T_1 mapping

Tianyi Ke[1]
Eun-Kee Jeong[2]
Xuli Wang[1]
Yi Feng[3]
Dennis L Parker[2]
Zheng-Rong Lu[1]

[1]Departments of Pharmaceutics and Pharmaceutical Chemistry; [2]Radiology and Materials Science and [3]Engineering, University of Utah, Salt Lake City, UT, USA

Abstract: Cyclic Arg-Gly-Asp-D-Phe-Lys [c(RGDfK)] targeted poly(*L*-glutamic acid) (PGA)-(Gd-DO3A) conjugate with a biodegradable cystamine spacer was prepared and evaluated for in vivo detection of an angiogenesis biomarker, $\alpha_v\beta_3$ integrin, in neoplastic tissues with T_1 mapping, a quantitative magnetic resonance imaging (MRI) technique. The binding activity of the c(RGDfK) containing conjugate was investigated using in vitro vitronectin assay with human prostate carcinoma DU145 cell line and Kaposi's sarcoma SLK cell line. The peptide c(RGDfK) and PGA-cystamine-(Gd-DO3A) conjugate were used as controls. The binding affinity of polymer bound c(RGDfK) was slightly lower than free c(RGDfK) peptide. The RGD targeted conjugate had higher binding affinity to the DU145 cells than the SLK cells, which was consistent to free c(RGDfK). The imaging of $\alpha_v\beta_3$ integrin with targeted PGA-cystamine-(Gd-DO3A) was evaluated in nude mice bearing DU145 and SLK xenografts at a dose of 5 μmol-Gd/kg. The targeted conjugate demonstrated higher in vivo binding affinity to the DU145 xenografts than the SLK xenografts, resulting in a significant decrease of T_1 values of water protons in the periphery of the DU145 tumors as shown in the MR T_1 maps. No significant decrease of T_1 values was observed in the SLK tumor with the targeted conjugate and in both tumors with the non-targeted conjugate. The targeted polymeric Gd(III) chelate conjugate with a degradable spacer has the potential to be a new paradigm for safe and effective probes in molecular imaging with quantitative MR T_1 mapping.

Keywords: MRI contrast agent, $\alpha_v\beta_3$ integrin, RGD, PGA-cystamine-(Gd-DO3A), MR T_1 mapping

Introduction

Excessive angiogenesis is involved in tumor proliferation and many other disorders. Noninvasive specific imaging of angiogenesis is critical for more accurate and earlier detection of angiogenic diseases and the assessment of antiangiogenic therapeutic efficacy. The $\alpha_v\beta_3$ integrin is one of several proteins involved in the angiogenic process and is a potent biomarker for angiogenesis. The $\alpha_v\beta_3$ integrin is highly expressed at the surface of proliferating endothelial cells in neoplastic and metastatic tissues (Brooks et al 1994). It is a viable molecular target for detecting angiogenesis and evaluating the efficacy of antiangiogenesis treatment (Haubner et al 2001; Achilefu et al 2005; Line et al 2005; Schmieder et al 2005). Contrast enhanced magnetic resonance imaging (MRI) can be effective for molecular imaging of the $\alpha_v\beta_3$ integrin if a sufficient amount of contrast agent is delivered to the target (Sipkins et al 1998).

Previously, we have conjugated Gd-DO3A to biocompatible poly(*L*-glutamic acid) (PGA) via a cleavable cystamine spacer to develop a safe and effective macromolecular MRI contrast agent (Lu et al 2003; Ke et al 2006). A large amount of Gd-DO3A chelates can be loaded onto the polymeric carrier. The degradable disulfide spacer can be

Correspondence: Zheng-Rong Lu
Department of Pharmaceutics and Pharmaceutical Chemistry, University of Utah, 421 Wakara Way, Suite 318, Salt Lake City, UT 84108, USA
Tel +1 801 587 9450
Fax +1 801 585 3614
Email zhengrong.lu@utah.edu

reduced by endogenous free thiols (eg, cysteine and reduced glutathione) to facilitate the excretion and to minimize the long-term body accumulation of toxic Gd(III) ions after the MRI study. Incorporation of an $\alpha_v\beta_3$ integrin specific targeting moiety to the polymer conjugate can result in a targeted macromolecular MRI contrast agent for in vivo detection of the biomarker with MRI.

We report here the synthesis and evaluation of an Arg-Gly-Asp (RGD) targeted PGA-cystamine-(Gd-DO3A) conjugate for in vivo detection of the $\alpha_v\beta_3$ integrin in neoplastic tissues with MR T_1 mapping. RGD is a peptide motif that can specifically bind to the $\alpha_v\beta_3$ integrin (Pasqualini et al 1997). T_1 mapping is a quantitative MRI technique and can accurately measure and map the T_1 values of water protons in organs and tissues. When the targeted polymer conjugate binds to the molecular target, it decreases the T_1 values of surrounding water protons. The overexpressed $\alpha_v\beta_3$ integrin can be visualized in the MR T_1 map where the T_1 values decrease significantly due to the binding of the targeted contrast agent.

Materials and methods

Poly(*L*-glutamic acid) (PGA) (M_w = 80.8 KDa, M_n = 69.1 KDa) was synthesized according to the literature (Idelson and Blout 1958). Mono-Boc-cystamine (Lu et al 2003) and N-succinimidyl bromoacetate (Callahan et al 1989) were prepared according to literature methods. Di-*tert*-butyl dicarbonate and 1-ethyl-3-(3-dimethylaminopropyl)carbodiimide hydrochloride (EDC) were purchased from Nova Chemicals (La Jolla, CA). 1,4,7,10-Tetraazacyclododecane (cyclen) was purchased from Macrocyclics (Dallas, TX). 1,4,7,10-Tetraazacyclododecane-1,4,7-trisacetic acid (DO3A) was synthesized according to a published method (Ke et al 2006). Bromoacetic acid, N-hydroxysuccinimide (NHS) and N-diisopropylethylamine (DIEA) were purchased from Lancaster Synthesis, Inc. (Pelham, NH). Gadolinium(III) acetate and *tert*-butyl bromoacetate were purchased from Alfa Aesar (Ward Hill, MA). Ethylenediaminetetraacetic acid (EDTA) dipotassium salt and cystamine dichloride were purchased from Sigma-Aldrich (St. Louis, MO). The peptide of cyclo{Arg-Gly-Asp-D-Phe-(ω-N-(N-(8-amino-3, 6-dioxaoctanoyl)-8-amino-3,6-dioxaoctanoyl)Lys)} was custom-made by Peptides International, Inc. (Louisville, KY). All chemicals were used without further purification. Spectra/Por® 6 membrane (MWCO: 25,000) was purchased from Spectrum Laboratory, Inc. (Rancho Dominguez, CA). Matrigel was purchased from BD Biosciences (San Jose, CA). Human prostate carcinoma DU145 cell line and Kaposi's sarcoma tumor SLK cell line were purchased from the ATCC collection (Manassas, VA, USA) and cultured in flasks in Modified Eagle's Minimum Essential medium (MEM) with 10% fetal bovine serum for DU145 cells and RPMI 1640 medium with 10% fetal calf serum for SLK cells.

NMR spectra were recorded at 25 °C on a varian INOVA 400 at 400MHz. ESI mass spectra were acquired on PE Sciex API III Mass Spectrometer. The molecular weights of the polymers were determined by size exclusion chromatography (SEC) on an AKTA FPLC system with a Superose 6 column equipped with UV and refractive index detectors (calibrated with poly[(N-2-hydroxypropyl)methacrylamide] standards). The Gd content in the conjugates was determined by inductively coupled plasma-optical emission spectroscopy (ICP-OES, Perkin-Elmer, Optima 3100XL, Norwalk, CT). Amino acid analysis was done on Beckmann 6300 ninhydrin-based system.

Synthesis of N-t-Boc-cystamine bromoacetamide

N-Succinimidyl bromoacetate (2.83 g, 12 mmol) was added to a solution of mono-N-*t*-Boc-cystamine (2.25 g, 10 mmol) in methylene chloride (50 ml) at 0 °C and the mixture was stirred overnight at room temperature. The reaction solution was washed with 1 M $NaHSO_4$ solution (3 × 30 ml) and dried over anhydrous $MgSO_4$. The product was isolated by flash chromatography with 3:1 hexane/ethyl acetate. Yield: 2.36 g (71%). ^{1}HNMR, δ_H ($CDCl_3$, ppm): 7.14 (1H, br, NHCO of bromoacetamide), 4.95 (1H, br, NHCO of Boc), 3.87 (2H, s, CH_2Br), 3.59 (2H, t, CH_2N near to bromoacetamide), 3.44 (2H, t, CH_2N near to Boc), 2.83 (2H, t, CH_2S near to bromoacetamide), 2.77 (2H, t, CH_2S near to Boc), 1.42 (9H, s, $(CH_3)_3C$–). ESI-MS (m/z, $M+H^+$): 373.1 (measured), 373.0 (calculated).

Synthesis of 1,4,7,10-tetraazacyclododecane-1,4,7-tris (acetic acid)-10-(acetic acid-cystamine monoamide) (I)

DO3A (0.7 g, 1.5 mmol) and N-Boc-cystamine bromoactamide (1.05 g, 3.0 mmol) were dissolved in a mixture of 14 mL methanol and 7 mL triethylamine. An excess of anhydrous K_2CO_3 was added to the solution. The reaction mixture was stirred overnight at room temperature and the solvent was then removed under vacuum. The residue was washed with ether and acetone, and then dissolved in 5 mL cold water in an ice bath. The solution was acidified to pH = 2~3 with 1N HCl, then concentrated to dryness under vacuum. The residue was washed using ether and acetone, and the product

was extracted from the solid residue with a mixed solvent of 14 mL methanol and 7 mL triethylamine. After the solvent was evaporated under vacuum, the residue was dissolved in 3 mL trifluoroacetic acid in ice bath and stirred for 15 minutes at room temperature to remove the Boc protection. Trifluoroacetic acid was evaporated under vacuum and the residue was washed with ether. The final product, a white solid, was collected and dried under vacuum. Yield: 0.91 g (60%). ^{1}HNMR, δ_H (D_2O, ppm): 3.34–3.69 (8H, m, CH_2CO of acetic acid and acetamide), 3.16–3.34 (4H, m, CH_2N of cystamine), 2.90–3.15 (16H, m, CH_2N of cyclen), 2.70–2.90 (4H, m, CH_2S of cystamine). ESI-MS (m/z, $M+H^+$): 539.3 (measured), 539.2 (calculated).

Synthesis of PGA-OSu ester

PGA (500 mg) and N-hydroxysuccinimide (2.5 g, excess) were dissolved in 20 mL anhydrous DMF. EDC (2.5 g) was then added to the solution. The reaction mixture was stirred for 3 days at room temperature, and then concentrated under vacuum. The residue was dropped into 30 mL anhydrous acetone to precipitate PGA-OSu active ester. The polymer was collected by filtration, washed with acetone and dried under vacuum. Yield: 867 mg (100%). 1HNMR, δ_H (d_6-DMSO, ppm): 8.25 (1H, br, NHCO), 4.18 (1H, br, NHCHCO), 2.40–3.20 (6H, m, CH2CO), 2.08 (2H, br, CH2).

Synthesis of PGA-cystamine-[Gd(III)-DO3A]-c(RGDfK) conjugate

PGA-OSu (40 mg), c(RGDfK) (30 mg, 0.026 mmol), and p-dimethylaminopyridine (216 mg, 1.77 mmol) were dissolved in 6 mL anhydrous DMF. The mixture was stirred for 2 h at room temperature and then compound I (212 mg, 0.21 mmol) was added into solution. The reaction mixture was stirred to react for 24 h at room temperature. The solution was then diluted with water in an ice bath and dialyzed against deionized water with Spectrra/Por® 6 membrane (molecular weight cutoff: 25,000 Da, Spectrum Laboratory, Inc). The polymeric ligand was then reacted with an excess of $Gd(OAc)_3$ (100 mg) overnight at room temperature in aqueous solution at pH 6. Xylenol orange indicator was then added, followed by EDTA until the pink color disappeared. The paramagnetic conjugate was purified by dialysis with Spectra/Por® 6 membrane and lyophilized. Yield: 42 mg (62%). The gadolinium content in the conjugate was 27 mol-%, as determined by ICP-OES. The content of c(RGDfK) was 13 mol-% by amino acid analysis, determined by the ratio of normalized concentration of D-phenylalanine to glutamic acid.

Synthesis of PGA-cystamine-[Gd(III)-DO3A]

PGA-cystamine-[Gd(III)-DO3A] was similarly prepared according to above described method without c(RGDfK). Yield: 70%. The gadolinium content was 20.8 mol-%, as determined by ICP-OES.

T_1 relaxivity measurement

T_1 relaxation times for the polymeric contrast agents of three concentrations and water were determined by sequential application of a standard inversion-recovery (IR) pulse sequence on a Siemen Trio 3T scanner. The parameters were 5000 ms repetition time (TR), 17 ms echo time (TE) and, 22, 25, 30, 35, 40, 50, 100, 200, 300, 400, 500, 600, 700, and 800 ms inversion time (TI). Net magnetization amplitude data for each sample were measured at regions of interest. T_1 and M_0 were calculated by fitting the Marquardt-Levenberg algorithm with multiparametric nonlinear regression (Liang and Lauterbur 2000; Mohs et al 2005). The relaxivity r_1 was calculated from the slop of the plot of $1/T_1$ vs [Gd (III)].

Binding assay of the conjugates

The binding activity of the c(RGDfK) in the targeted polymeric contrast agent was studied in an $\alpha_v\beta_3$ integrin dependent adhesion assay according to a reported method (Kok et al 2002; Schmieder et al 2005). Briefly, flat bottom 96-well culture plates were coated overnight with vitronectin (500 ng/well in PBS) at 4 °C. After washing with PBS, the wells were incubated with 1% bovine serum albumin (BSA) for 2 h at 37 °C to block nonspecific binding and washed two times with PBS. The DU 145 and SLK cells were trypsinized and resuspended in serum free MEM at a concentration of 2×10^5 cells/mL. Aliquots (100 μL) of cell suspensions and serum free MEM (blank) or solutions of c(RGDfK), PGA-cystamine-(Gd-DO3A)-c(RGDfK) and PGA-cystamine-(Gd-DO3A) were mixed and incubated for 15 min at 4 °C. The concentrations of c(RGDfK) were 5 μM or 50 μM for both c(RGDfK) and PGA-cystamine-(Gd-DO3A)-c(RGDfK). The concentration of PGA-cystamine-(Gd-DO3A) was the same as PGA-cystamine-(Gd-DO3A)-c(RGDfK) based on the Gd content. The mixtures were then plated at 2×10^4 cells/well (200 μL) and allowed to adhere for 24 h at 37 °C. The unattached cells were removed from the wells by washing five times with PBS. The attached cells were fixed with 3.7% paraformaldehyde for 30 minutes at room temperature, washed twice with PBS and stained with 0.1% crystal violet (50 μL/well) at

25 °C for 30 min. Excess dye was removed by washing with deionized water and 0.2% Triton-X (50 μL/well) was added to extract dye absorbed by adherent cells. Absorbance was measured at 575 nm on a Molecular Devices Spectra Max M2 microplate reader (Sunnyvale, CA). The results were normalized to the control.

Animal tumor model

Male athymic nude mice (25–30 grams, 8 weeks old, Animal Production Program of National Cancer Institute at Frederick, Frederick, MD) were cared under the guidelines of an approved protocol from the University of Utah Institutional Animal Care and Use Committee. A suspension of DU 145 cells in the MEM or SLK cells in the RPMI-1640 medium at 2×10^7 cells/mL was mixed with an equal volume of Matrigel (Becton-Dikinson, Franklin Lakes, NJ). The Matrigel mixtures of DU145 cells and SLK cells (2×10^6 cells in 200 μL) were subcutaneously implanted into the upper left and right flanks of the mice, respectively. Tumors in both flanks reached 0.5–1.5 cm in diameter three weeks post-inoculation and were ready for experiment.

Dynamic T_1 mapping

Mice bearing tumor xenografts were anesthetized by intraperitoneal administration of a mixture of ketamine (45 mg/kg) and xylazine (6 mg/kg). The contrast agents were injected via a tail vein at a dose of 5.0 μmol-Gd/kg. A group of three mice was used for each conjugate. The MRI data were acquired on a Siemens Trio 3T MRI system (Siemens Medical Solution, Erlangen, Germany). High-resolution MR images of the mice was acquired before and 8 minutes after the injection of contrast agents using a 3D FLASH sequence with 0.5 mm^3 isotropic resolution, 128 × 64 × 48 imaging matrix, 7.5 ms TR, 2.7 ms TE, and 4 signal averages. The imaging time was 1 min 30 sec. T_1 mapping source images were acquired using a spoiled gradient-echo pulse sequence with 128 × 64 imaging matrix, 300 ms TR, 1.75 ms TE, and flip angles 10, 20, 30 and 45º. The in-plane resolution was 1.0 × 1.0 mm^2 with 2.0 mm slice thickness. Data acquisition duration for each flip angle and 8 slices was 15 sec. Since T_1 mapping with flip angle variations is very sensitive to the RF field variation, mouse was positioned with tumor tissues located near the center of the RF coil. The dynamic images for T_1 mapping were processed pixel-by-pixel for all time points by custom software using IDL (Interactive Data Language, Boulder, CO) to construct the T_1 maps. For calculating the longitudinal relaxation time T_1, the signal intensities were fitted according to the following equation (Deoni et al 2003):

$$\frac{S_{FLASH}(\vec{r};TR,\alpha)}{\sin\alpha} = E_1 \cdot \frac{S_{FLASH}(\vec{r};TR,\alpha)}{\tan\alpha} + M_o(1-E_1)$$

where $E_1 = (1-e^{-TR/T_1(\vec{r})})$; $S(\vec{r};TR,\alpha)$ is the measured signal intensity for a flip angle with the fixed TR, at the position.

Statistical analysis

Statistical analysis was performed using the t-test (GraphPad Prism; GraphPad Software, San Diego, CA). P values were two-tailed with a confidence interval of 95%. Difference was considered significant when $p < 0.05$.

Results

The RGD targeted poly(*L*-glutamic acid)-(Gd-DO3A) conjugate was synthesized by stepwise conjugation of DO3A cystamine monoamide (I) and a pentameric cyclic peptide c(Arg-Gly-Asp-D-Phe-Lys) [c(RGDfK), II] to poly-(*L*-glutamic acid) N-hydroxysuccinimide ester (PGA-NHS), followed by complexation with $Gd(OAc)_3$, Scheme 1. The c(RGDfK) peptide was first conjugated to PGA via a long spacer N-(8-amino-3,6-dioxaoctanoyl)-8-amino-3,6-dioxaoctanoic acid (ADAD), which was designed to minimize the steric hindrance of the polymer chain for RGD to bind with its target. EDTA was used to remove the excess Gd(III) ions bound to the carboxylic groups of PGA. PGA-cystamine-(Gd-DO3A) conjugate was similarly prepared as a control agent. The physicochemical parameters of two conjugates are listed in Table 1. The content of c(RGDfK) in the targeted conjugate was approximately 13 mol-%, as determined by ^1H NMR spectrometry before Gd complexation and by amino acid analysis after complexation. The gadolinium content was approximately 27 mol-%, as determined by ICP-OES. The T_1 relaxivity of the targeted and non-targeted conjugates was 9.7 and 8.2 $mM^{-1}s^{-1}$ per complexed Gd(III) ion at 3 Tesla, respectively. The apparent molecular weights of the conjugates were different from those of the starting polymers because of the decrease in hydrodynamic volumes of the polymers after conjugation.

Table1 Physical chemical parameters of PGA-cystamine-(Gd-DO3A) and PGA-cystamine-(Gd-DO3A)-c(RGDfK) conjugates

Property	PGA-cystamine-(Gd-DO3A)	PGA-cystamine-(Gd-DO3A)-c(RGDfK)
M_w (KDa)	79.3	49
M_w/M_n	1.81	1.89
Gd content, (w/w)%[b]	12.14	9.27
Molar conjugation ratio	20.8	27
R_1 ($mM^{-1}s^{-1}$)	7.8	9.7

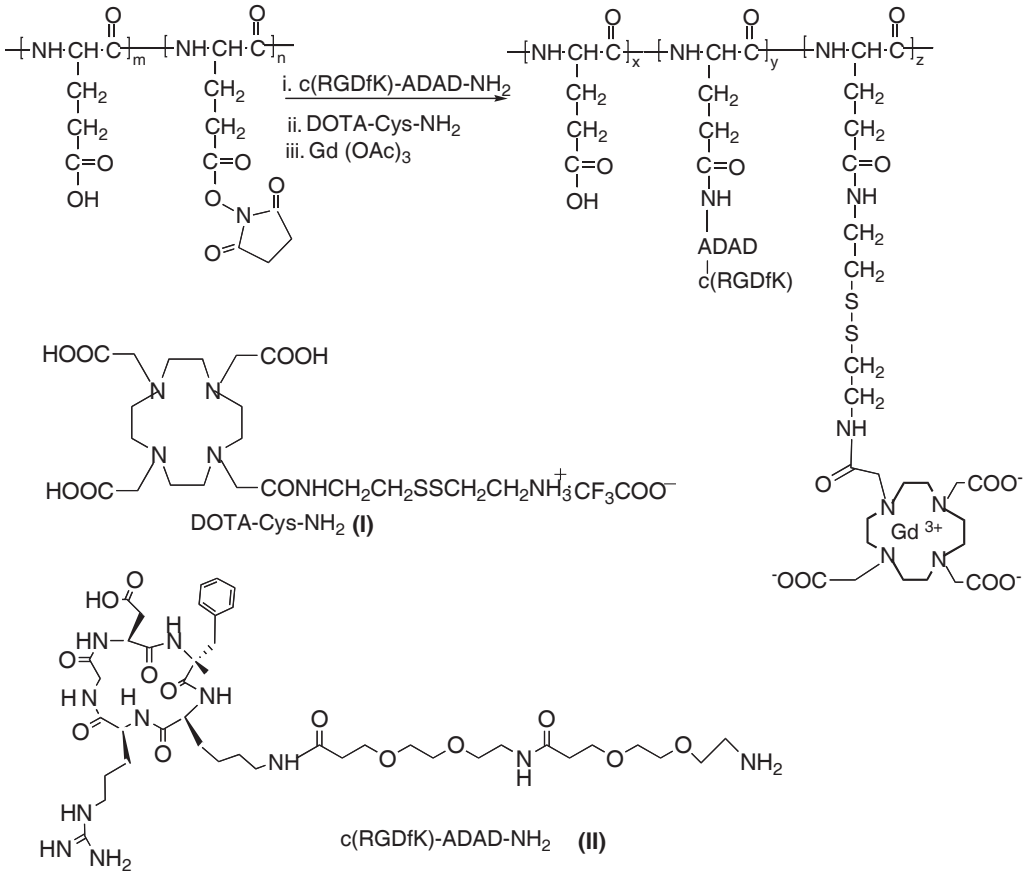

Scheme 1 Synthesis of RGD containing PGA-cystamine-(Gd-DO3A); i. DMAP, DMF, rt, 2 h; ii. DMAP, DMF, rt, 24 h. iii. $Gd(OAc)_3$, Na_2-EDTA, pH 5.5, rt, 24 h.

The binding activity of the c(RGDfK) containing conjugate was investigated by an in vitro vitronectin assay with the human prostate carcinoma DU145 cell line and Kaposi's sarcoma SLK cell line. The c(RGDfK) peptide and PGA-cystamine-(Gd-DO3A) conjugate were used as controls. The $\alpha_v\beta_3$ integrin is expressed on the surface of both DU145 (Romanov and Goligorsky 1999) and SLK cells (Samaniego et al 2002). Figure 1 shows the inhibition of cell attachment to vitronectin–coated plates by the agents. Both c(RGDfK) and the c(RGDfK) containing conjugate exhibited stronger concentration-dependent inhibition for the DU145 cells than the SLK cells. The percentages of cell attachment for free c(RGDfK) and conjugated c(RGDfK) at 50 μM were 3.4 ± 3.8% ($p < 0.01$ when compared with the control) and 14 ± 4.9% ($p < 0.01$) for the DU145 cells, and 25 ± 17.4% ($p < 0.01$) and 56 ± 9% ($p < 0.01$) for the SLK cells, respectively. The percentages of cell attachment for free c(RGDfK) and conjugated c(RGDfK) at 5 μM were 34 ± 8.2% ($p < 0.01$) and 53 ± 5% ($p < 0.01$) for the DU145 cells, and 54 ± 6.5 ($p < 0.05$) and 67 ± 20.3% ($p = 0.15$) for the SLK cells, respectively. The non-targeted conjugate did not have significant effect on cellular adherence inhibition ($p > 0.05$) for both cell lines at both 5 and 50 μM. The results showed the c(RGDfK) in the conjugate maintained the affinity to the $\alpha_v\beta_3$ integrin after conjugation.

Figure 2 shows the coronal MR images of tumor bearing mice before and at 8 minutes after injection of the conjugates at a dose of 5 μmol-Gd/kg. The low dose was used to effectively evaluate the targeting efficiency by minimizing non-specific accumulation of the polymeric agents in tumor tissues. Both conjugates resulted in signal enhancement in the liver and blood. No significant enhancement was observed in both DU145 and sarcoma tumors for the targeted conjugate and control conjugate. Conventional MRI was not sensitive enough to detect the binding of the targeted contrast agent in the tumor tissue.

Figure 3 shows color-coded T_1 maps before and at 9.5 and 17.5 minutes after the injection of the contrast agents. The maps show that the tumor tissues had relatively higher T_1 values as compared to the surrounding tissue. The targeted conjugate resulted in a significant decrease of T_1 values at the tumor periphery of the DU145 xenografts, which had a high binding

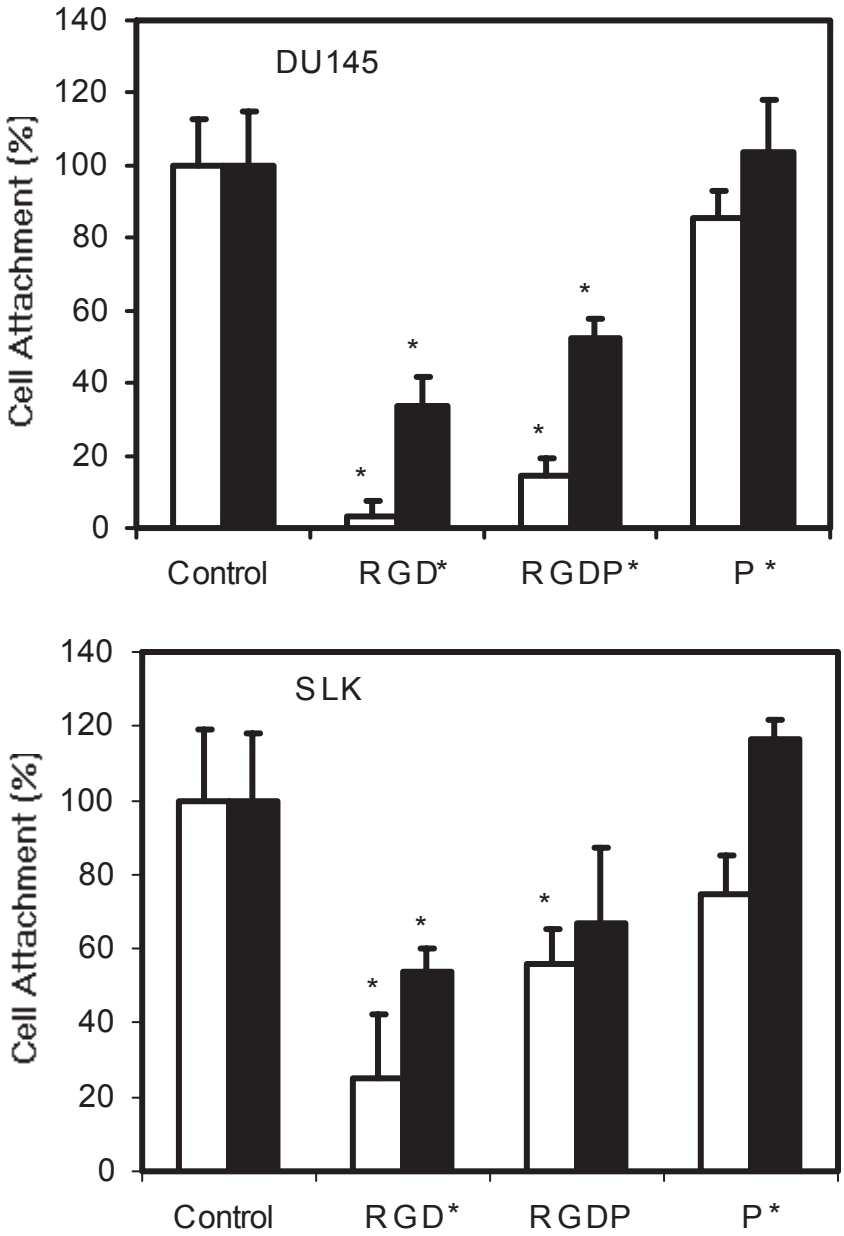

Figure 1 Percentage of cell attachment of human prostate carcinoma DU145 cells and Kaposi's sarcoma SLK cells to the vitronectin-coated plates inhibited by MEM serum free media (control) or solutions of c(RGDfK) (RGD), c(RGDfK) containing PGA-cystamine-(Gd-DO3A) (RGDP), and PGA-cystamine-(Gd-DO3A) (P) at the concentrations of 5 μM (closed bar) and 50 μM (open bar). Values are shown as means ± SD (n = 5). The "*" symbol indicates $p < 0.05$. The comparison is made to the control.

activity to the targeted conjugate. No significant change of the T_1 values was found in DU-145 tumor with the non-targeted agent and the SLK tumor for both conjugates. Quantitative T_1 measurement was more sensitive to detect the binding of the targeted conjugate in different tumors than conventional MRI.

Discussion

Magnetic resonance imaging is less sensitive for molecular imaging than nuclear medicine. A relatively large amount of Gd(III) chelates is required in order to generate detectable signals to visualize molecular targets. Biocompatible polymeric conjugates are effective drug delivery systems for both therapeutics and diagnostics. A large amount of Gd(III) chelates can be loaded onto the conjugates, and targeting agents can also be incorporated to develop targeted MRI contrast agents. The biodegradable disulfide spacer allows release of Gd(III) chelates from the conjugates, facilitating rapid excretion of the Gd(III) chelates after the imaging studies (Wang et al 2005; Feng et al 2006). Rapid excretion and minimal retention of Gd(III) chelates are critical for clinical application of the targeted polymer paramagnetic conjugates. Targeted polymeric Gd(III) chelate conjugates

with a biodegradable spacer have a potential for in vivo molecular imaging with MRI.

The RGD targeted PGA-cystamine-(Gd-DO3A) conjugate had a relatively high load of Gd(III) chelates. A high RGD content was incorporated into the conjugate to achieve multi-functionality and effective in vivo targeting. The in vitro binding studies demonstrated that the RGD targeted conjugate was effective for targeting the $\alpha_v\beta_3$ integrin. The c(RGDfK) peptide had higher binding affinities in the DU145 cells than in SLK cells ($p < 0.03$ at both 5 and 50 μM). The binding affinity of polymer bound c(RGDfK) was lower than free c(RGDfK) ($p < 0.03$), which is possibly due to the steric effect of the polymer chains. The RGD targeted conjugate had higher binding affinity to the DU145 cells as compared with the SLK cells ($p = 0.31$ at 5 μM and $p < 0.01$ at 50 μM), consistent to c(RGDfK) affinity.

A very low dose (5.0 μM-Gd/kg) was used to avoid nonspecific tissue interactions of the conjugates for in vivo imaging of the $\alpha_v\beta_3$ integrin. The dose of macromolecular MRI contrast agents for effective tumor MR imaging are generally in the range of 0.03–0.1 mmol-Gd/kg. Such a high dose could saturate the binding to the molecular target in the tumor tissues and generate a strong background signal due to nonspecific tumor accumulation. However, conventional MR imaging does not have sufficient sensitivity to detect the changes in signal intensity around the molecular targets with very low concentration of Gd(III) chelates. As shown in Figure 2, no significant enhancement was observed in the tumors after injection of both targeted and nontargeted conjugates as compared with the precontrast images. Signal intensity in MRI is generated by the combination of longitudinal (T_1) and transverse (T_2) relaxations of water protons. Gd(III) chelate increases both longitudinal ($1/T_1$) and transverse ($1/T_2$) relaxation rates of water protons. The increase in the relaxation rate ($1/T_1$) is proportional to the concentration of Gd(III) chelate, resulting in bright signal in MR images. However, the contrast agent also significantly increases T_2 and T_2* relaxation rate, resulting in reduction of MR signal intensity, which could supersede the signal increase caused by increasing T_1 relaxation rate. Consequently, no significant increase in signal intensity was observed in the tumor tissues on the MR images with conjugates at a very low dose.

T_1 mapping directly measures the T_1 values of tissues and can accurately determine the changes in the relaxation time caused by paramagnetic complexes. Since T_1 relaxation rate ($1/T_1$) is linearly correlated to the concentration of the contrast agents, T_1 mapping has a potential to quantitatively determine biomarkers with targeted MRI contrast agents.

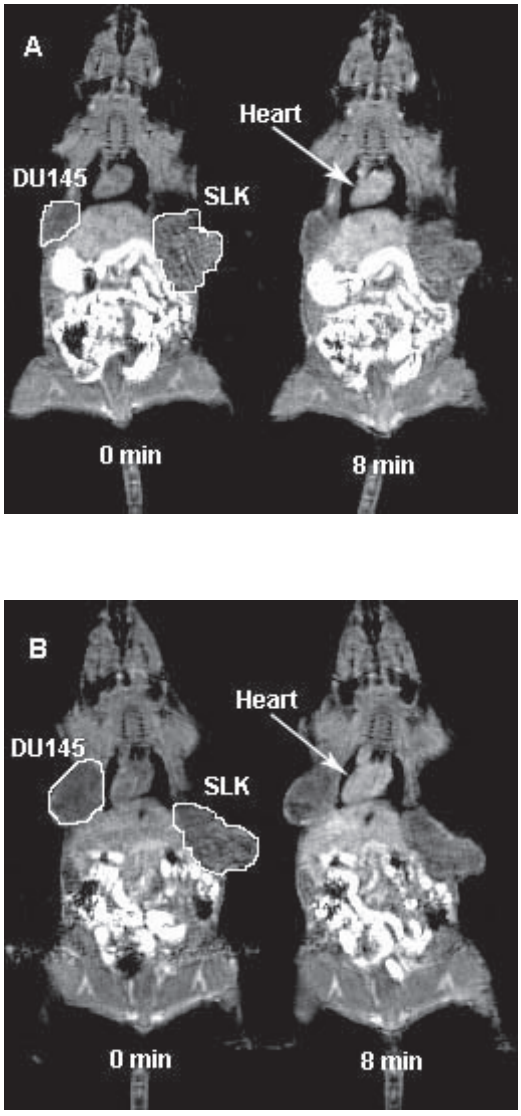

Figure 2 T_1-weighted contrast enhanced coronal MR images of mice bearing human prostate carcinoma DU145 (left flank) and Kaposi's sarcoma SLK (right flank) xenografts before and at 8 minutes after injection of the c(RGDfK) containing PGA-cystamine-(Gd-DO3A) conjugate (A) and PGA-cystamine-(Gd-DO3A) (B).

A decrease in T_1 values was observed in the periphery of DU145 tumor after the injection of the targeted conjugate on the color-coded T_1 maps, while no obvious changes in the T_1 values were found in the core of DU145 tumor, Figure 3. No significant decrease in T_1 values was observed for the nontargeted agent in DU-145 tumor and for both conjugates in the SLK tumor in the T_1 maps. The results indicate that the targeted conjugate with high binding affinity to the DU145 cells resulted in significant T_1 reduction at the tumor periphery due to specific binding to the biomarker $\alpha_v\beta_3$ integrin. High T_1 values inside the tumor tissue for the targeted conjugate might be attributed to tumor necrosis and inefficient delivery of the agent to the inner tumor

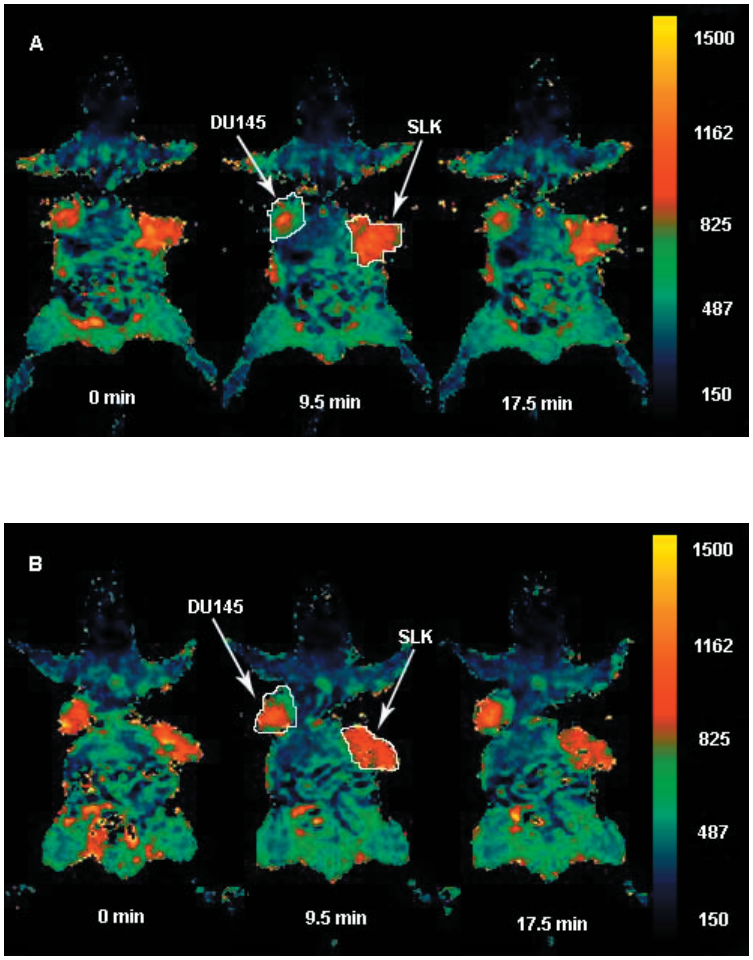

Figure 3 T_1 maps of mice bearing human prostate carcinoma DU145 (left flank) and Kaposi's sarcoma SLK (right flank) xenografts before and after injection of the c(RGDfK) containing PGA-cystamine-(Gd-DO3A) conjugate (A) and PGA-cystamine-(Gd-DO3A) (B).

tissue (Padera et al 2004). Specific binding of the targeted conjugate to the SLK tumor tissue was trivial and nonspecific accumulation of the nontargeted conjugate in both tumors was minimal. Consequently, no significant reduction of T_1 values was observed for the targeted conjugate with low binding affinity in the SLK tumor and for the nontargeted conjugate in both tumors.

The RGD targeted PGA-cystamine-(Gd-DO3A) conjugate was effective for targeting the angiogenesis biomarker, $\alpha_v\beta_3$ integrin, and quantitative T_1 mapping was more sensitive for detecting the bound targeted agent than conventional T_1-weighted MRI. The RGD targeted PGA-cystamine-(Gd-DO3A) was able to specifically deliver a large amount of Gd-DO3A to the target, resulting in detectable T_1 shortening with T_1 mapping. Since a very low dose was used, the nonspecific accumulation of the polymer conjugate in the solid tumor was minimized leading to reduced background MR signal, and allowing the detection of T_1 shortening in the tissue with high expression of the $\alpha_v\beta_3$ integrin. However, the load of Gd(III) chelates to the PGA polymer conjugate was still relatively low. The efficacy of targeted paramagnetic polymer conjugate can be further improved for MR molecular imaging if the loading efficiency of the Gd(III) chelate to the polymer carrier is improved.

In conclusion, the conjugation of the RGD peptide to PGA-cystamine-(Gd-DO3A) maintained its binding affinity to $\alpha_v\beta_3$ integrin. The targeted conjugate had a high binding affinity to human prostate carcinoma DU145 cell line and was effective for the detection of the angiogenesis biomarker $\alpha_v\beta_3$ integrin in the DU145 tumor with quantitative T_1 mapping. Targeted polymeric Gd(III) chelate conjugate with a biodegradable spacer can be a new paradigm for safe and effective probes in MR molecular imaging.

Acknowledgment

We are grateful for the technical support from Dr. Yongen Sun and Ms. Melody Johnson. The work was supported in part by NIH grant CA097465.

References

Achilefu S, Bloch S, Markiewicz MA, et al. 2005. Synergistic effects of light-emitting probes and peptides for targeting and monitoring integrin expression. *Proc Natl Acad Sci U S A*, 102:7976–81.

Brooks PC, Clark RAF, Cheresh DA. 1994. Requirement of vascular integrin $\alpha_v\beta_3$ for angiogenesis. *Science*, 264:569–71.

Callahan JF, Ashton-Shue D, Bryan HG, et al. 1989. Structure-activity relationships of novel vasopressin antagonists containing C-terminal diaminoalkanes and (aminoalkyl)guanidines. *J Med Chem*, 32:391–6.

Deoni SCL, Rutt BK, Peters TM. 2003. Rapid combined T_1 and T2 mapping using gradient recalled acquisition in the steady state. *Magn Reson Med*, 49:515–26.

Feng Y, Zong Y, Ke T, et al. 2006. Pharmacokinetics and blood pool contrast enhancement of Gd-DTPA Cystine Copolymers and Gd-DTPA Cystine Diethyl Ester Copolymers. *Pharm Res*, 23:1736–42.

Haubner R, Wester HJ, Weber WA, et al. 2001. Noninvasive imaging of $\alpha_v\beta_3$ integrin expression using 18F-labeled RGD-containing glycopeptide and positron emission tomography. *Cancer Res*, 61:1781–5.

Idelson M, Blout ER. 1958. Polypeptides. XXI. High molecular-weight poly (α, L-glutamic acid): preparation and optical rotation changes. *J Am Chem Soc*, 80:4631–4.

Ke T, Feng Y, Guo J, et al. 2006. A Biodegradable cystamine spacer facilitates the clearance of Gd (III) chelates in poly (glutamic acid) Gd-DOTA conjugates for contrast enhanced MR imaging. *Magn Reson Imaging*, 24:931–40.

Kok RJ, Schraa AJ, Bos EJ, et al. 2002. Preparation and functional evaluation of RGD-modified proteins as $\alpha_v\beta_3$ integrin directed therapeutics. *Bioconjugate Chem*, 13:128–35.

Liang Z-P, Lauterbur PC. 2000. Principle of magnetic resonance imaging. New York: IEEE Pr.

Line BR, Mitra A, Nan A, et al. 2005. Targeting tumor angiogenesis: comparison of peptide and polymer-peptide conjugates. *J Nucl Med*, 46:1552–60.

Lu ZR, Wang X, Parker DL, et al. 2003. Poly(*L*-glutamic acid) Gd(III)-DOTA conjugate with a degradable spacer for magnetic resonance imaging. *Bioconjugate Chem*, 14:715–19.

Mohs AM, Zong Y, Guo J, et al. 2005. PEG-g-poly(GdDTPA-co-L-cystine): effect of PEG chain length on in vivo contrast enhancement in MRI. *Biomacromolecules*, 6:2305–11.

Padera TP, Stoll BR, Tooredman JB, et al. 2004. Pathology: Cancer cells compress intratumor vessels. *Nature*, 427:695.

Pasqualini R, Koivunen E, Ruoslahti E. 1997. Alpha v integrins as receptors for tumor targeting by circulating ligands. *Nat Biotechnol*, 15:542–6.

Romanov VI, Goligorsky MS. 1999. RGD-recognizing integrins mediate interactions of human prostate carcinoma cells with endothelial cells in vitro. *The Prostate*, 39:108–18.

Samaniego F, Young D, Grimes C, et al. 2002. Vascular endothelial growth factor and Kaposi's sarcoma cells in human skin grafts. *Cell Growth Differ*, 13:387–95.

Schmieder AH, Winter PM, Caruthers SD, et al. 2005. Molecular MR imaging of melanoma angiogenesis with 3-targeted paramagnetic nanoparticles. *Magn Reson Med*, 53:621–7.

Sipkins DA, Cheresh DA, Kazemi MR, et al. 1998. Detection of tumor angiogenesis in vivo by $\alpha_v\beta_3$-targeted magnetic resonance imaging. *Nature Med*, 5:623–6.

Wang X, Feng Y, Ke T, et al. 2005. Pharmacokinetics and long-term Gd tissue accumulation of (Gd-DTPA)-cystamine copolymers, a biodegradable macromolecular MRI contrast agent. *Pharm Res*, 22:596–601.